Recent Development of 5 V Cathode Materials for Lithium Rechargeable Batteries

Hyun-Soo Kim[†], Padikkasu Periasamy*, and Seong-In Moon

Korea Electrotechnology Research Institute, Changwon 641-120, Korea
*Central Electrochemical Research Institute, Karaikudi-630 006, Tamil Nadu, India

Abstract : This paper deals with the recent development of high-voltage cathode materials of mono- and di- metal ions substituted spinel $LiMn_2O_4$ for lithium batteries. $LiCu_xMn_{2-x}O_4$ ($0 \leq x \leq 0.5$) shows reversible intercalation/deintercalation in two potential regions, 3.9~4.3 and 4.8~5.0 V, and stable electrochemical cycling behavior but with low capacity. $LiNi_{0.5}Mn_{1.5}O_4$ obtained by a sol-gel process delivers a capacity of 127 mAh g^{-1} on the first cycle and sustains a value of 124 mAh g^{-1} even after the 60th cycle. The $Li_xCr_yMn_{2-y}O_4$ ($0 \leq x \leq 1.0$) solid-solutions exhibit enhanced specific capacity, larger average voltage, and improved cycling behaviors for low Cr content. $LiCr_yMn_{2-y}O_4$ presents a reversible Li deintercalation process at 4.9 V, whose capacity is proportional to the Cr content in the range of $0.25 \leq x \leq 0.5$ and delivers higher capacities. $LiM_yCr_{0.5-y}Mn_{1.5}O_4$ (M=Fe or Al) shows that the capacity retention is lowered compared with lithium manganate. The cumulative capacities obtainable with Al-substitutted materials are less than those with Fe-substituted materials. $LiCr_xNi_{0.5-x}Mn_{1.5}O_4$ (x=0.1) delivers a high initial capacity of 152 mAh g^{-1} with excellent cycleability.

Key words : Cathode material, 5 V, High voltage, Capacity retention, Lithium rechargeable battery

1. Introduction

High energy density, high rate capability, low weight, safe, low cost, and long cycle life are strongly needed for various large-scale applications such as self-powering micro electronics components, portable electronics and electric vehicles.[1] Among competing devices, rechargeable lithium batteries show the highest energy density due to the high reducing power of lithium that leads to high voltage for the cell. The limitations in the overall performance of lithium batteries depend on both the intrinsic performances of the materials (cathode, anode and electrolyte) and the technological aspects (material processing, electrode fabrication, and battery conception), taking into account the environment of each material in the complete cell. A amount of work has been done worldwide in these two directions over the last twenty years. Currently, $LiCoO_2$ is the preferred electrode material for commercial lithium-ion batteries, which are now being manufactured at a rate of more than 250 million units/year. Nonetheless, Co and Ni compounds have economic and environmental problems that leave the door open to exploit alternative materials.

Cathode materials for rechargeable lithium cells must posses several desirable properties such as high specific energy, good electrochemical rechargeability, good electronic conductivity, high lithium diffusivity, and chemical compatibility with the electrolyte. For these above reasons, the major

emphasis of this effort has been directed towards identifying candidate cathode electrode materials. Only three lithiated materials with high operating voltage are presently known i.e., $LiCoO_2$, $LiNiO_2$ and $LiMn_2O_4$.

Recently, spinel $LiMn_2O_4$ and its derivatives have generated great interest as promising cathode materials for lithium batteries due to their low cost, abundance and non-toxicity compared with Co and Ni oxides.[2-5] This paper deals with the recent development of 5 V cathode materials of mono- and di- metal ions substituted spinel $LiMn_2O_4$ for lithium batteries.

2. Compounds doped with single metal-ions

2.1. $Li(M_{0.5}Mn_{1.5})O_4$ [M = Co, Fe, Ni, Cu, Ti, Cr and Zn]

For $Li(M_{0.5}Mn_{1.5})O_4$ [M = Co, Fe, Ni, Cu, Ti, Cr and Zn], LiOH, MnO, TiO_2, Cr_2O_3, FeOOH, $Co(OH)_2$, $Ni(OH)_2$, CuO or Zn $(OH)_2$ was used as raw materials, the mixed reactants (Li : Me : Mn = 2 : 1 : 3 in molar ratio) were typically pressed into pellets and heated at 550°C for 15 h in air. These pre-calcined materials were then ground and again pressed into pellets, which were subsequently reacted at 750°C for 15 h in air.[6]

The results of slow scan voltammetry for (a) Li/$LiCr_{0.5}Mn_{1.5}O_4$, (b) Li/$LiMn_{0.5}Mn_{1.5}O_4$, (c) Li/$LiFe_{0.5}Mn_{1.5}O_4$, (d) Li/$LiCo_{0.5}Mn_{1.5}O_4$, (e) Li/$LiNi_{0.5}Mn_{1.5}O_4$, and (f) Li/$LiCu_{0.5}Mn_{1.5}O_4$ at rate of 0.2 mVs^{-1} in 1 M $LiPF_6$ EC+DEC (1 : 1 vol%) are shown in Fig. 1. As can be seen in Fig. 1, the chromium-, iron-, cobalt-, nickel- and copper- containing sample with a spinel structure based on lithium, manganese
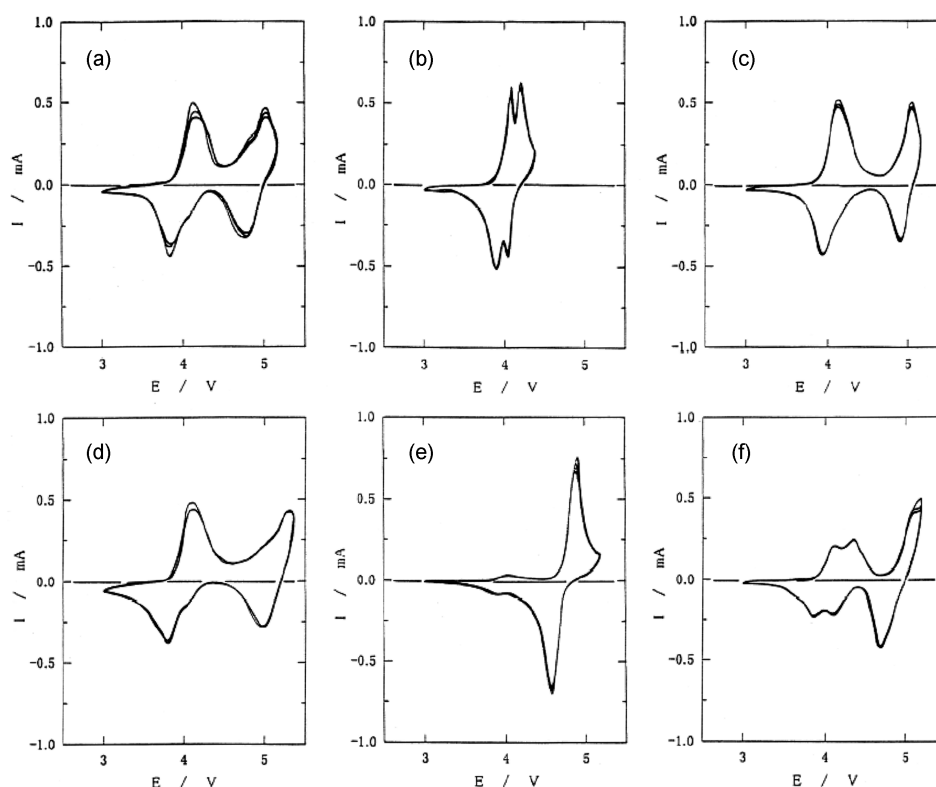
Fig. 1. Slow-scan voltammetry of Li/Li[Me$_{1/2}$Mn$_{3/2}$]O$_4$ cells (Me : (a) Cr, (b) Mn, (c) Fe, (d) Co, (e) Ni, or (f) Cu at a rate of 0.2 mVs^{-1} in 1.0 M LiPF$_6$/EC : DEC (1:1 vol %).
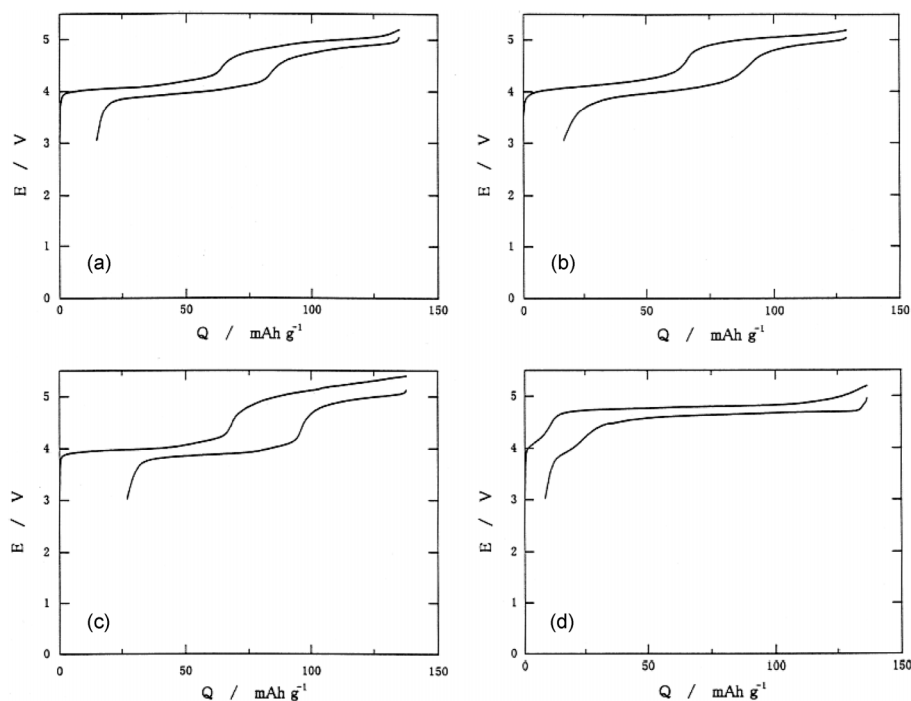

Fig. 2. Charge and discharge curves of (a) Li/Li[Cr$_{1/2}$Mn$_{3/2}$]O$_4$, (b) Li/Li[Fe$_{1/2}$Mn$_{3/2}$]O$_4$, (c) Li/Li[Co$_{1/2}$Mn$_{3/2}$]O$_4$, and (d) Li/Li[Ni$_{1/2}$Mn$_{2/3}$]O$_4$ cells operated in voltages above 3 V at a rate of 0.2 mA cm^{-2}. Electrode area was 3 cm^2 (1.5 × 2.0 cm^2).

and oxygen gives operating voltage higher than 4.5 V in addition to normal operating voltage around 4 V. Of these, Ni doped LiMn$_2$O$_4$ appears differently when it compares with other materials. The first charge-discharge curves of (a) Li/ LiCr$_{0.5}$Mn$_{1.5}$O$_4$, (b) Li/LiFe$_{0.5}$Mn$_{1.5}$O$_4$, (c) Li/LiCo$_{0.5}$Mn$_{1.5}$O$_4$ and (d) Li/LiNi$_{0.5}$Mn$_{1.5}$O$_4$ cells operated in a voltages range

of 3.05.2 V at a rate of 0.2 mA cm^{-2} are shown in Fig. 2. $LiNi_xMn_{2-x}O_4$ shows predominantly one-step reaction at 4.8 V while other materials show approximately two-step reactions at 4.0 and 5.0 V. The decrease of capacity during the first charge and discharge is in the following order: Ni < Cr < Cu < Fe < Co, which is the same as that in operating voltage order. This indicates that the decrease of capacity is mainly due to electrolyte decomposition, which occurs above 4.8 V. The longer the electrodes exposed at higher voltages, the larger decrease of the capacity.

2.2. $LiCu_xMn_{2-x}O_4$

$LiCu_xMn_{2-x}O_4$ ($0.1 \leq x \leq 0.5$) cathode materials were prepared by conventional solid state method. In the solid-state synthesis, $LiOH \cdot H_2O$ was mixed intimately with the required amounts of CuO and MnO_2 for a given stoichiometry and then heated at 750°C for 18 hrs in air.[7]

Fig. 3 shows the charge-discharge curves for a Li/$LiCu_xMn_{2-x}O_4$ ($0 \leq x \leq 0.5$) cell cycled between 3.3 to 5.1 V. The electrolyte composition was 1.2 M $LiPF_6$ in a mixture of EC and DMC in a volume ratio of 2 : 3. This electrolyte was selected because of its reported stability to oxidation up to 5 V. The total capacity of $LiCu_xMn_{2-x}O_4$ electrodes drops with increasing copper content from 119 mAh g^{-1} at x = 0.1 to 71 mAh g^{-1} at x = 0.5. Table 1 summarizes the relative capacities obtained in the high voltage region (5.1~4.5 V) and low voltage region (4.5~3.3 V).

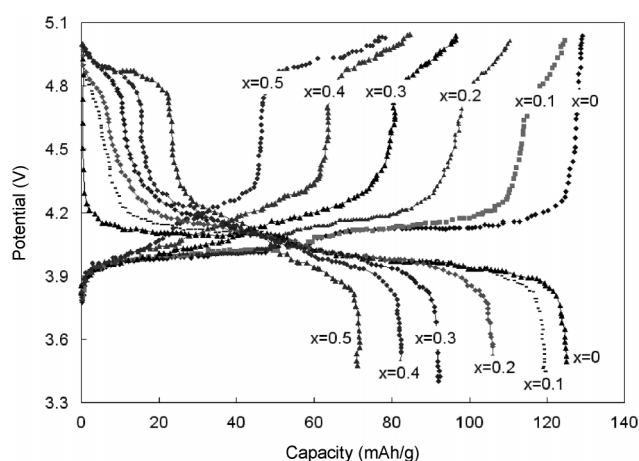Fig. 4 shows the cycling performance in terms of charge-discharge capacity between 5.1 and 3.3 V, expressed in mAh g^{-1} vs cycle number for the series of $LiCu_xMn_{2-x}O_4$ electrodes. The available capacity decreased as the amount of copper in the series increases. However, electrodes with higher copper content showed significantly improved capacity retention during cycling. For example $Li/LiCu_{0.1}Mn_{1.9}O_4$ cells show on average, an initial capacity of 120 mAh g^{-1} which decreases to 103 mAh g^{-1} after 70th cycles, reflecting a 14% decrease, where as $Li/LiCu_{0.5}Mn_{1.5}O_4$ cells show an initial capacity of 71 mAh g^{-1} that fades to 65 mAh g^{-1} over the same cycle number (8% decrease). Some capacity decrease may be attributed to electrolyte oxidation.

Novel electro-active materials $LiCu_xMn_{2-x}O_4$ ($0.1 \leq x \leq 0.5$) have been prepared and evaluated in the lithium cells. The data show that lithium can be extracted from the spinel structures in two main potential regions: 3.9~4.3 and 4.8~5.0 V, attributed to the oxidation of Mn^{3+} to Mn^{4+} and Cu^{2+} to Cu^{3+}, respectively. The reactions are reversible. Stable electrochemical cycling has been observed for electrode compositions with high values of x (x = 0.5, $LiCu_{0.5}Mn_{1.5}O_4$) but with low capacity (60~70 mAh g^{-1}).

2.3. $LiNi_{0.5}Mn_{1.5}O_4$

Spinel $LiNi_{0.5}Mn_{1.5}O_4$ was prepared from a mixture of manganese acetate, nickel nitrate and lithium hydroxide using a sol-gel method. Sample was prepared by firing the dry gel first at 600°C for 12 h and annealing at 850°C for 24 h in air.[8]

The first charge-discharge curves for a Li/$LiNi_{0.5}Mn_{1.5}O_4$ fired at 850°C cell cycled between 3.5 and 4.9 V with a current density of 0.5 mA cm^{-2} in 1.0 M $LiPF_6$ dissolved in PC are shown in Fig. 5. The cell delivered a capacity of 114 mAh g^{-1} at 4.66 V plateau and 127 mAh g^{-1} in total during the initial cycle. This value is much larger than that previously reported data[2]: i.e., about 90 mAh g^{-1} at 4.7 V plateaus. On the other hand, the first charge capacity of the cell is lower than that of previously reported data by about 20 mAh g^{-1}, which indicates that there is less electrolyte decomposition. Materials fired at 850°C have regular shape with well-defined crystal

Fig. 3. Potential-capacity curves obtained from the third cycle for $LiCu_xMn_{2-x}O_4$ (0 = x = 0.5) in 1.2 M $LiPF_6$/EC : DMC (2 : 3 vol %).

Table 1. Relative capacities of $LiCu_xMn_{2-x}O_4$ (0.1 = x = 0.5) electrodes.

x in $LiCu_xMn_{2-x}O_4$	Capacity at 5.14.5 V (mAh g^{-1})	Capacity at 4.53.3 V (mAh g^{-1})
X = 0.1	7	112
X = 0.2	10	96
X = 0.3	13	79
X = 0.4	19	63
X = 0.5	23	48

Fig. 4. Cycle life behavior of $LiCu_xMn_{2-x}O_4$ (0 = x = 0.5) in 1.2 M $LiPF_6$ / EC : DMC (2 : 3 vol %).
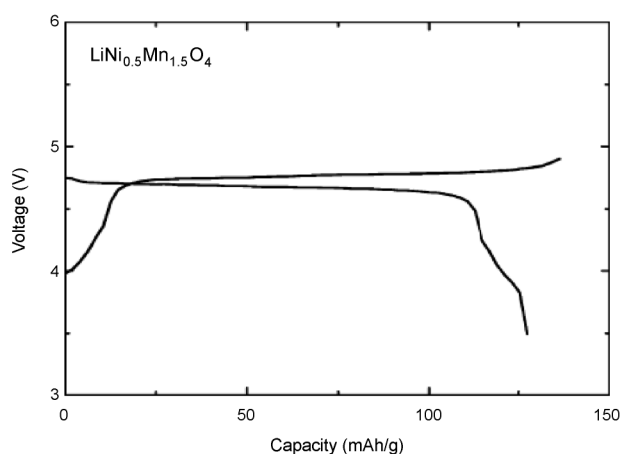
Fig. 5. First charge-discharge curves for Li/LiNi$_{0.5}$Mn$_{1.5}$O$_4$ cell at a current density of 0.5 mA cm^{-2} in voltage range of 3.5~4.9 V in LiPF$_6$/PC.

Fig. 7. Voltage profiles for Li/LiNi$_{0.5}$Mn$_{1.5}$O$_4$ cell as a function of different discharge rate. Current densities are (1) 0.25 mA cm^{-2}, (2) 0.5 mA cm^{-2}, (3) 1.0 mA cm^{-2}, (4) 1.5 mA cm^{-2} and (5) 2.0 mA cm^{-2}.
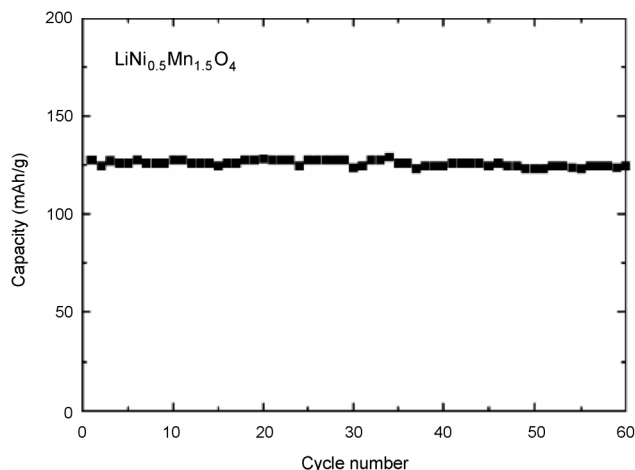

Fig. 6. Discharge capacity vs. cycle number for Li/LiNi$_{0.5}$Mn$_{1.5}$O$_4$ cell at a current density of 0.5 mA cm^{-2} in voltage range of 3.5~4.9 V in LiPF$_6$/PC.

Fig. 8. Cyclic voltammograms for Li/LiNi$_{0.5}$Mn$_{1.5}$O$_4$ cell at a scan rate of 0.05 mV s^{-1}: (1) pristine cell, (2) after 30th cycles at a current density of 0.5 mA cm^{-2}.

phases, whereas the particles of the material fired at 600ºC are flat and loosely connected particles.

A plot of discharge capacity versus cycle number for a cell of the material fired at 850ºC and cycled at 0.5 mA cm^{-2} is given in Fig. 6. After 60th cycles, the total discharge capacity was still above 124 mAh g^{-1}. This value is better than those of previously obtained: i.e., 80 mAh g^{-1} on the 16th cycle and 105 mAh g^{-1} on the 32nd cycle, respectively. The rate performance of the same material during discharge is presented in Fig. 7. The corresponding Li/LiNi$_{0.5}$Mn$_{1.5}$O$_4$ cells deliver 128, 127, 121, 108, and 100 mAh g^{-1} at a current density of 0.25, 0.5, 1.0, 1.5, 2.0 mA cm^{-2}, respectively. It is clear that the material gives similar rate performance at current densities 0.5 mA cm^{-2}. The voltammetric behavior, which obtained at a scan rate of 0.05 mVs^{-1} after the 1st and 30th cycles, of a LiNi$_{0.5}$Mn$_{1.5}$O$_4$ electrode is compared in Fig. 8. Three reversible couples appear and are related to the various phase tran-
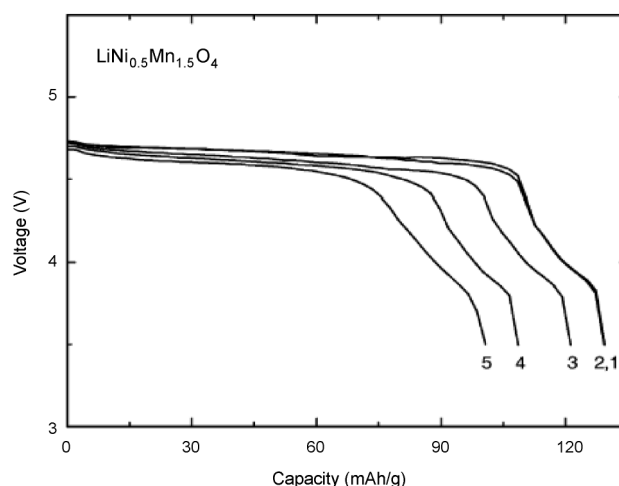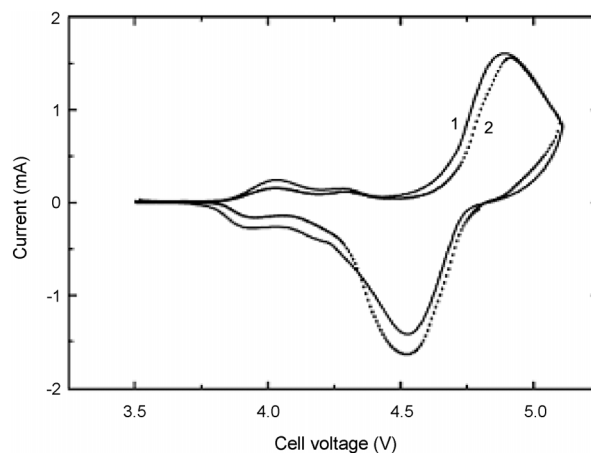
sitions between the intercalation stages. The small peaks around 4.0 V are related to the redox couple Mn^{3+}/Mn^{4+} and its redistribution in the spinel as in the case of undoped LiMn$_2$O$_4$, while the large peaks as higher voltage correspond to the redox couple Ni^{2+}/Ni^{4+}. These peaks illustrate well the reversibility of this material upon deintercalation and intercalation of lithium ions over the potential range 3.5~5.1 V versus Li/Li$^+$. On the other hand, the negligible decrease in peak height with cycling is in agreement with the quite small decrease in capacity shown by the cycling performance curve presented in Fig. 6. The sol-gel procedure endows sample with higher crystallinity. The material delivers a capacity of 127 mAh g^{-1} on the first cycle and sustains a value of 124 mAh g^{-1} even after 60 cycles.

2.4. LiCr$_y$Mn$_{2-y}$O$_4$ (0 ≤ y ≤ 1.0)

LiCr$_y$Mn$_{2-y}$O$_4$ materials were prepared from mixture of the

reactants lithium carbonate, manganese carbonate, and chromium carbonate in stoichiometric proportions. The mixtures were heated at 750°C for 24 h in air and subjected to two successive and identical grinding and annealing treatments.

Fig. 9 shows the voltage versus capacity curves obtained for different Cr contents in $Li/LiCr_yMn_{2-y}O_4$ cells (y = 0, 0.25, 0.5, 0.75) during the charge at C/6 and the discharge at C/15 up to 5.4 V. The electrolyte used in these studies was 1.0 M $LiPF_6$ dissolved in 2:1 (vol%) mixture of EC:DMC. Li intercalation occurs in two main steps, at 4.9 V and at 4.0 V. As a matter of fact, the capacity of the 4 V process decreases with increasing chromium content, in agreement with the literature,[10] but a new intercalation process is observed at about 4.9 V, whose capacity increases with increasing chromium content in the range of 0.25 to 0.75. The $LiMn_2O_4$ material showed a much lower capacity than the other members of the solid solution.[11]

Fig. 10 shows the cyclic behaviors of various $Li_xCr_yMn_{2-y}O_4$ material cells. It can be seen from Fig. 10, two main behaviors were observed according to the chromium content: i.e., satis-

Fig. 9. First discharge curves at C/15 of $Li_xCr_yMn_{2-y}O_4$ after an initial charge at C/6 up to 5.4 V.

Fig. 10. Relative capacity variation up on cycling of $Li_xCr_yMn_{2-y}O_4$ materials (charge at C/6 and discharge at C/15)

factory cycleability for y = 0.5 and low capacity for y = 0.75. A lower capacity decrease upon cycling is observed for y = 0.25 compared to the non-substituted $LiMn_2O_4$ material, which indicates that low manganese to chromium substitution is beneficial to the cyclability of the materials. For y = 0.75, the capacity fading is very fast, probably due to an irreversible structural change in the spinel structure upon deintercalation/intercalation reactions.

The $Li_xCr_yMn_{2-y}O_4$ (0 < y < 1.0) solid solutions exhibit improved electrochemical properties such as enhanced specific capacity, larger average voltage, and improved cycling behaviors for low Cr content. But for high Cr contents, the cycleability becomes very poor. This drastic influence of the Cr composition on the Li insertion behavior has been attributed to a structural evolution. At high Cr content, transition metal cations migrate from the 16d sites to the tetrahedral 8a sites and octahedral 16c sites of the spinel structure upon cycling, which blocks more and more 8a sites, that can no longer be accessible to Li^+ ions. The improved cycleability observed for low Cr contents as compared to pure $LiMn_2O_4$ is believed to come from a lower variation of the unit cell volume during the intercalation-deintercalation process.

3. Compounds doped with double metal-ions

3.1. $LiM_yCr_{0.5-y}Mn_{1.5}O_4$ (M = Fe or Al)

The substituted compounds, $LiM_yCr_{0.5-y}Mn_{1.5}O_4$ (M = Fe or Al; y = 0.0, 0.1, 0.2, 0.3 and 0.4), were synthesized by a solid-state fusion method from oxide, carbonate and hydroxide precursors. Stoichiometric amounts of Li_2CO_3, MnO_2, and Cr_2O_3 and the desired substitution compound, Fe_2O_3 or $Al(OH)_3$, were thoroughly ground in an agate mortar and palletized. The pellets were then fired in a muffle furnace at 800°C for 24 h in air. After cooling to room temperature, the pellets were ground again.[12]

The cyclic voltammograms were recorded between 3.00 and 5.01 V in 1.0 M $LiPF_6$/EC:DEC (1:1 vol%) solution. Although electrolyte might decomposed at the higher voltage, no evidence for any decomposition could be seen in the voltammograms. In fact, $LiPF_6$-based electrolytes, such as the one used in this study, are fairly tolerant to high voltages. The cyclic voltammograms recorded for the doped systems in Figs. 11(a) and (b) show two regions of electrochemical activity. One around 4.0 V, corresponding to the lithium intercalation/deintercalation into/from the 8a tetrahedral sites and associated with the Mn^{4+}/Mn^{3+} couple, and the other above 4.5 V, corresponding to the oxidation/reduction of the substitutions ion (Cr, Fe or Al). Fig. 11(b) showed that, in $LiFe_{0.1}Cr_{0.4}Mn_{1.5}O_4$, an oxidation peak at 4.15 V corresponding to the oxidation of Mn^{3+} to Mn^{4+}, and a broad peak at 5.04 V with a prominent shoulder at 4.85 V, while the peak at 5.04 V is attributable to the oxidation of Fe^{3+} to Fe^{4+}, and the reaction corresponding to the shoulder at 4.85 V is due to the Cr^{4+}/Cr^{3+} couple. At lower Cr levels, such as $LiFe_{0.4}Cr_{0.1}Mn_{1.5}O_4$ shown in Fig. 11(a), the shoulder at 4.85 V apparently vanishes, indicating that the contribution from the Cr^{4+}/Cr^{3+} couple is not significant. However, the 5-V peak shifts to 5.09 V.
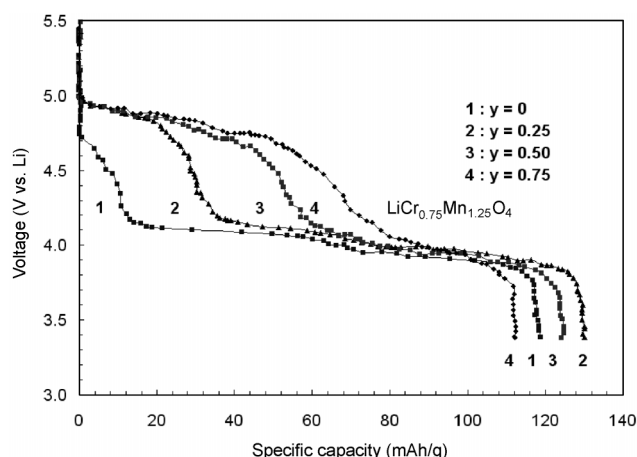
Fig. 11. Cyclic voltammograms of (a) LiFe$_{0.4}$Cr$_{0.1}$Mn$_{1.5}$O$_4$; (b) LiFe$_{0.1}$Cr$_{0.4}$Mn$_{1.5}$O$_4$. at a scan rate of 0.1 mV s^{-1}.

Fig. 12. Cycling performance of LiM$_y$Cr$_{0.5-y}$Mn$_{1.5}$O$_4$: (a) M = Fe; (b) M = Al. Chargedischarge rate: 0.1 C.

The corresponding reduction peak also shifts to 4.80 to 4.90 V. It is also seen from Fig. 11 (a) and (b) that an increase in the Fe content from 0.1 to 0.4 resulted not only in a shift of the redox potential of the Mn^{4+}/Mn^{3+} couple but also in an increase in the currents associated with the redox peaks. Thus, Fe as a substitutent seems to influence the electrochemical characteristics of the Mn^{4+}/Mn^{3+} couple.

Fig. 12 (a) and (b) were depicted the cycling behavior of cells with Fe- and Al-substituted LiM$_y$Cr$_{0.5-y}$Mn$_{1.5}$O$_4$ compositions rate in the electrolyte 1.0 M solution of LiPF$_6$ in EC : DEC (1 : 1 vol%). It can be seen from Fig. 12(a) that when 0.1 molecule of Fe was introduced, capacity at the first cycle rose to 117 mAh g^{-1}. However, an increase in the Fe content

from 0.1 to 0.4 in LiFe$_y$Cr$_{0.5-y}$Mn$_{1.5}$O$_4$ reduced discharge capacity of the first cycle from 117 to 109 mAh g^{-1}. The corresponding values at the 40th cycle were 88 and 70 mAh g^{-1}, with charge retentions of 75 and 64%, respectively. Thus, as the Fe content increased, not only was there a decrease in the deliverable capacity, there was also diminished capacity retention. In other words, the replacement of the octahedral site stabilizing Cr with Fe resulted in decreased stability of the spinel framework.

Similarly, in the case of LiAl$_y$Cr$_{0.5-y}$Mn$_{1.5}$O$_4$, a gradual decrease in the capacity at the first cycle more Cr was substituted with Al. It can be seen from Fig. 12(b) that as the Al stoichiometry was increased from 0.1 to 0.4, the capacity of the first cycle decreased from 112 to 103 mAh g^{-1}. However, these values were lower than the corresponding values obtained with Fe as a co-substitutent. Obviously, Fe being a transition metal lends itself to oxidation-reduction reactions, accounting for part of the capacity. The discharge capacities recorded in the 40th cycle with LiAl$_y$Cr$_{0.5-y}$Mn$_{1.5}$O$_4$ were 82 and 67 mAh g^{-1} for y = 0.1 and y = 0.4, respectively. The corresponding values for capacity retention were 73 and 66% respectively. Simultaneous substitution of LiMn$_2$O$_4$ with Cr and Al shows that an increase in Al content reduces both discharge capacity and cycling stability.

In conclusion, despite the fact that the reversible capacities in the 4 V region for the doped compositions were lower than that for the undoped LiMn$_2$O$_4$ (Table 2), the decrease of capacity in the 4 V region is more than made up in the 5 V region. Therefore, the cumulative capacity was higher than the capacity of undoped compound. Additionally, the capacities around the higher voltage region represent the higher specific energy of the spinel materials. Simultaneous substitution of Cr and Fe or Cr and Al for Mn in the LiMn$_2$O$_4$ spinel was attempted with an aim of developing stable and high voltage cathode materials. In this regards, increased the amount of substitution Fe or Al to the lithium chromium manganate electrodes, both the capacity retention was lower compared with lithium manganate. The cumulative capacities obtainable

Table 2. The initial capacities of the various substituted materials.

No.	Composition	4 V capacity (mAh g^{-1})	5 V capacity (mAh g^{-1})	Total capacity (mAh g^{-1})
1	$LiMn_2O_4$	108.0	-	108.0
2	$LiCr_{0.5}Mn_{1.5}O_4$	75.1	38.9	114.0
3	$LiFe_{0.1}Cr_{0.4}Mn_{1.5}O_4$	81.0	36.0	117.0
4	$LiFe_{0.2}Cr_{0.3}Mn_{1.5}O_4$	83.0	32.0	115.0
5	$LiFe_{0.3}Cr_{0.2}Mn_{1.5}O_4$	83.4	30.7	114.1
6	$LiFe_{0.4}Cr_{0.1}Mn_{1.5}O_4$	85.5	23.5	109.0
7	$LiAl_{0.1}Cr_{0.4}Mn_{1.5}O_4$	77.2	37.8	115.0
8	$LiAl_{0.2}Cr_{0.3}Mn_{1.5}O_4$	86.2	25.8	112.0
9	$LiAl_{0.3}Cr_{0.2}Mn_{1.5}O_4$	87.9	21.1	109.0
10	$LiAl_{0.4}Cr_{0.1}Mn_{1.5}O_4$	88.9	14.1	103.0

with Al-substitutted materials were less than those with Fe-substituted materials.

3.2. $LiCr_xNi_{0.5-x}Mn_{1.5}O_4$

$LiCr_xNi_{0.5-x}Mn_{1.5}O_4$ (x = 0, 0.1, 0.3) powders were prepared by a sol-gel method using glycolic acid as a chelating agent. Lithium acetate, chromium nitrate, nickel acetate and manganese acetate were dissolved in distilled water, and added drop wise to a continuously stirred aqueous solution of glycolic acid. The resultant solution was evaporated at 70~80°C until a transparent sol and gel were obtained. The resulting gel precursors were decomposed at 450°C for 5 h in air and calcined at 900°C for 15 h in air.[13] The chromium- and nickel-doped spinel, $LiCr_xNi_{0.5-x}Mn_{1.5}O_4$ (x = 0, 0.1, 0.3) powders were each found to have a well defined spinel structure without any impurity phase by XRD.

Charge-discharge curves (10th cycles) for $LiCr_xNi_{0.5-x}Mn_{1.5}O_4$ (x = 0.0, 0.1, 0.3) electrodes in 1 : 2 (vol%) mixture of EC : DMC containing 1.0 M $LiPF_6$ are presented in Fig. 13. The charge-discharge cycle was performed galvanostatistically at a current density of 0.4 mA cm^{-2} between 5.2 and 3.5 V. The chromium-free $LiNi_{0.5}Mn_{1.5}O_4$ electrode has a very flat discharge plateau at 4.7 V versus Li/Li$^+$. It is well known that the 4.7 V plateau is ascribed to the oxidation of Ni^{2+}/Ni^{4+}. The 4.9 V plateau appears for the chromium- and nickel-doped $LiCr_xNi_{0.5-x}Mn_{1.5}O_4$ (x = 0.1, 0.3) electrode. With increasing Cr content, the capacity associated with the 4.7 V plateau decreases, while that resulting from the 4.9 V plateau increases.

The variation of discharge capacity as a function of cycle number for the $LiCr_xNi_{0.5-x}Mn_{1.5}O_4$ (x = 0.0, 0.1, 0.3) electrodes is given in Fig. 14. $LiCr_{0.1}Ni_{0.4}Mn_{1.5}O_4$ electrode delivers an initial discharge capacity of 152 mAh g^{-1} with excellent capacity retention, while the $LiNi_{0.5}Mn_{1.5}O_4$ electrode has a capacity of 141 mAh g^{-1} (x = 0). As can be seen from Fig. 14, the discharge capacity falls to 146 mAh g^{-1} as Ni further replaces Cr to form $LiCr_{0.3}Ni_{0.2}Mn_{1.5}O_4$ (x = 0.3). All three electrodes maintain their initial discharge capacities after extended cycling. The improvement in discharge capacity following the partial replacement of Ni with Cr can be attributed largely to the stabilization of the spinel structure and an
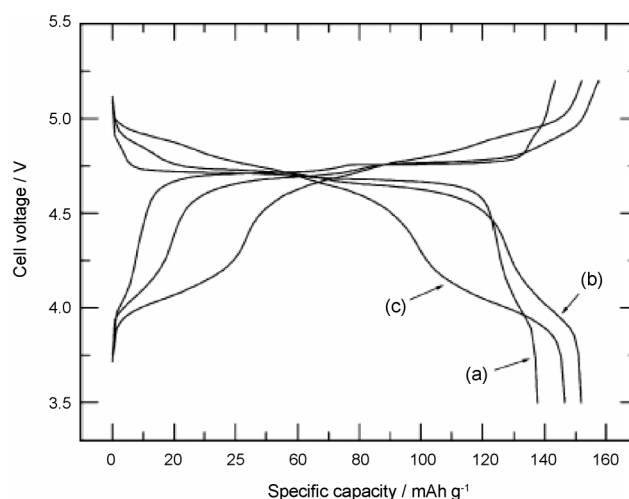

Fig. 13. Chargedischarge curves (10th cycle) for Li/LiCr$_x$Ni$_{0.5-x}$Mn$_{1.5}$O$_4$ cells in voltage range of 3.5~5.2 V: (a) x = 0; (b) x = 0:1; (c) x = 0:3.
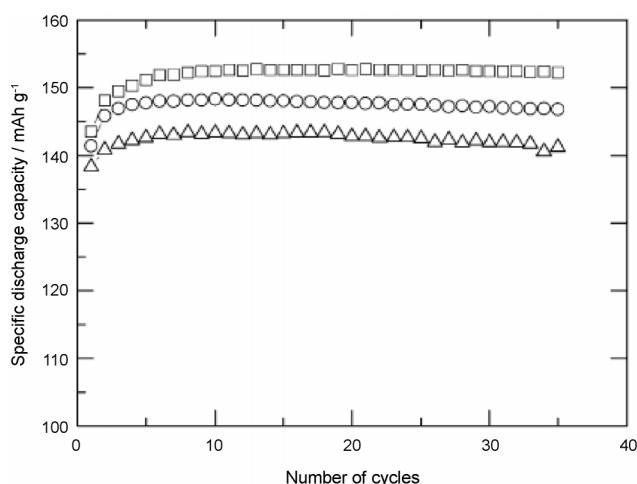

Fig. 14. Variation of specific discharge capacity as a function of cycle number for Li/LiCr$_x$Ni$_{0.5-x}$Mn$_{1.5}$O$_4$ cells: (a) x = 0; (b) x = 0:1; (c) x = 0:3.

increase in theoretical capacity due to the low molecular weight of Cr compared with that of Ni. In addition, the strength of the Cr-O bond is another reason for the improved capacity retention of the Cr- and Ni- doped $LiCr_{0.1}Ni_{0.4}Mn_{1.5}O_4$ electrode because the bonding energy of Cr-O (427 kJ mol^{-1}) is stronger than that of Mn-O (402 kJ mol^{-1}) and Ni-O (391.6 kJ mol^{-1}). The stronger Cr-O bond can stabilize the spinel structure by assisting retention of the local symmetry during cycling.

The discovery of highly oxidation resistant electrolyte compositions allows studying insertion compounds up to charging voltages higher than 5 V. Up to now, it has been found that substituted spinels $LiM_yMn_{2-y}O_4$ (Ni, Cu, Cr, Al and Fe) show reversible Li deintercalation capacities above 4.5 V. Some capacity is lost at 4 V for substituted spinels with the general formulation $LiM_yMn_{2-y}O_4$ (Ni^{2+}, Cr^{3+} and Cu^{2+}),

due to the lowering of the initial Mn^{3+} content. The missing capacity can be recovered at higher voltage. $LiCr_yMn_{2-y}O_4$ solid solution presents a reversible Li deintercalation process at 4.9 V, whose capacity is proportional to the Cr content in the range (y = 0.25-0.5) delivered higher capacities, i.e., 130 mAh g^{-1} due to Cr^{3+} to Cr^{4+}. $LiNi_yMn_{2-y}O_4$ (y = 0.5) materials deintercalate at 4.7 V, corresponding to Ni^{2+} to Ni^{4+} oxidation. $LiNi_{0.5}Mn_{1.5}O_4$ delivers about 100 mAh g^{-1}. The capacity above 4.5 V increased above 110 mAh g^{-1} with simultaneous Ni and Cr substitution in $LiCr_{0.1}Ni_{0.9}Mn_{1.5}O_4$.

4. Summary

Novel active materials, $LiCu_xMn_{2-x}O_4$ (0.1 = x = 0.5), show that lithium can be extracted reversibly from the spinel structures in two main potential regions: 3.9~4.3 V and 4.8~5.0 V, attributed to the oxidation of Mn^{3+} to Mn^{4+} and Cu^{2+} to Cu^{3+}, respectively. Stable electrochemical cycling has been observed for electrode compositions with high values of x ($LiCu_{0.5}Mn_{1.5}O_4$) but with low capacity (60~70 mAh g^{-1}). $LiNi_{0.5}Mn_{1.5}O_4$ obtained by a sol-gel process delivers a capacity of 127 mAh g^{-1} on the first cycle and sustains a value of 124 mAh g^{-1} even after 60 cycles. The $Li_xCr_yMn_{2-y}O_4$ ($0 \leq y \leq 1.0$) solid solutions exhibit improved electrochemical properties such as enhanced specific capacity, and larger average voltage, and improved cycling behaviors for low Cr content. The improved cyclability observed for low Cr contents as compared to pure $LiMn_2O_4$ is attributed by lower variation of the unit cell volume during the intercalation de-intercalation process.

$LiM_yCr_{0.5-y}Mn_{1.5}O_4$ (M = Fe or Al) was prepared in order to develope stable and high-voltage cathode materials. In this regards, increased the amount of substitution Fe or Al to the lithium chromium manganate electrodes, both the capacity retention was lower compared with lithium manganate. The

cumulative capacities obtainable with Al-substitutted materials were less than those with Fe-substituted materials. $LiCr_yMn_{2-y}O_4$ presents a reversible Li deintercalation process at 4.9 V, whose capacity is proportional to the Cr content in the range (0.25 $\leq$ y $\leq$ 0.5) delivered higher capacities i.e., 130 mAh g^{-1} due to Cr^{3+} to Cr^{4+}. $LiNi_yMn_{2-y}O_4$ (y = 0.5) materials deintercalate at 4.7 V, corresponding to Ni^{2+} to Ni^{4+} oxidation. $LiNi_{0.5}Mn_{1.5}O_4$ delivers the largest capacity of about 100 mAh g^{-1}. The capacity above 4.5 V increased above 110 mAh g^{-1} with the help of simultaneous Ni and Cr substitution in $LiCr_{0.1}Ni_{0.4}Mn_{1.5}O_4$.

References

1. M. Wakihara and O. Yamamota, *Lithium-ion batteries - Fundamental and performance*, Wiley-VCH, Weinheim, p. 26. (1997).
2. H. Kawai, M. Nagata, H. Tukamoto, Anthony R. West, *J. Power Sources*, **81-82** (1999) 67.
3. L. Hernan, J. Morales , L. Sanchez, and J. Santos, *Solid State Ionics*, **118** (1999) 179.
4. Y. Idemoto, H. Narai, and N. Koura, *J. Power Sources*, **119-121** (2003) 125.
5. Y. Terada, K. Yasaka, F. Nishikawa, T. Konishi, M.Yoshio, and I. Nakai, *J. Solid State Chem.*, **156** (2001) 286.
6. T. Ohzuku, S. Takeda and M. Iwanaga, *J. Power Sources*, **81-82** (1999) 90.
7. Y. Ein-Eli, S. Lu, W. Howard, S. Mukerjee, J. McBreen, J. Vaughey, and M. Thackeray, *J. Electrochem. Soc.*, **145** (1998) 1238.
8. X. Wu and S. Kim, *J. Power Sources*, **109** (2002) 53.
9. Q. Zhong, A. Bonakdarpour, M. Zhang, Y. Gao, and J. R. Dahn, *J. Electrochem. Soc.*, **144** (1997) 205.
10. J. M. Tarascon, E. Wang, W. R. Mckinnon and S. Colson, *J. Electrcochem. Soc.*, **138** (1991) 2859.
11. C. Sigala, D. Guyomard, A. Verbaere, Y. Piffard, and M. Tournoux, *Solid State Ionics*, **81** (1995) 167.
12. G. Fey, C. Lu and T. Kumar, *Materials Chemistry and Physics*, **80** (2003) 309.
13. K. Hong, Y. Sun, *J. Power Sources,* **109** (2002) 427.